Thermodynamic and Reactivity Parameters of Anions of Enol form of Isatin and its Halogenated Derivatives: A Theoretical Study

Esha Arora[1], Sunita Gulia[2]
[1]*Department of Chemistry, Shyama Prasad Vidyalaya Lodi Estate, New Delhi-110003*
[2]*Department of ICT & Training, Central Institute of Educational Technology, National Council of Educational Research and Training, Sri Aurobindo Marg, New Delhi-110016*

Abstract-This work presents the *first systematic DFT investigation of the enol-derived anionic forms of halogenated isatin derivatives*, encompassing mono- and dihalogen substitution at multiple ring positions. Unlike previous studies focused primarily on neutral isatins or isolated anionic species, this research provides a comprehensive analysis of stability, thermochemistry, and global reactivity trends for an entire family of halogenated isatin anions. These insights bridge a critical knowledge gap and offer a theoretical foundation for designing isatin-based frameworks with tunable reactivity for applications in medicinal chemistry, organic synthesis, and functional materials. The anionic forms of isatin and its halogen-substituted derivatives were systematically investigated using density functional theory (B3LYP/6-311++G) to elucidate their structural, electronic, and thermodynamic characteristics. Relative energy analysis reveals that halogenation markedly stabilizes the isatin anion, with bromine-substituted species—particularly those substituted at the C-9 and C-11 positions—exhibiting the lowest energy and greatest conformational flexibility. Thermochemical parameters (ΔH° and ΔG°) further confirm that anion formation becomes increasingly favorable as halogen electronegativity decreases, with dibromo derivatives demonstrating the highest thermodynamic preference for deprotonation. Global reactivity descriptors derived from conceptual DFT provide deeper insight into substituent-induced electronic modulation: halogen substitution narrows the HOMO–LUMO gap, enhances electrophilicity, and reduces nucleophilicity, reflecting stronger electron-withdrawing effects and increased reactivity. The combined analysis of structural, thermochemical, and electronic features reveals clear trends in stability and reactivity governed by halogen identity and substitution pattern. These findings contribute valuable theoretical understanding of isatin-based anions and offer a rational framework for designing halogenated isatin derivatives with tailored properties for applications in organic synthesis, medicinal chemistry, and functional material development.**

Keywords: Density Functional Theory (DFT); Global reactivity descriptors; Halogen substitution; Isatin derivatives; Molecular stability; Thermochemical parameters.

I. INTRODUCTION

Isatin (1H-indole-2,3-dione) is a versatile heterocyclic compound that has garnered significant interest in various fields of chemical research, including medicinal chemistry, organic synthesis, and materials science **[1–4]**. The presence of a rigid indole skeleton with two adjacent carbonyl functionalities at positions 6 and 7 endows isatin with unique structural features and a rich reactivity profile **[5–7]**. In particular, halogen-substituted derivatives of isatin further expand its chemical landscape by introducing electronic and steric modifications that can substantially influence reactivity, stability, and molecular interactions **[8–10,19–20]**. While the neutral forms of isatin and its halogenated analogs are well-studied **[1,5,8,19]**, their corresponding anionic forms remain comparatively underexplored **[11–13,16–18]**. Understanding the properties of these anions is essential for elucidating mechanistic pathways in reactions, optimizing synthetic strategies, and designing novel compounds with specific functional properties **[12–14,18]**.

From a medicinal chemistry standpoint, the isatin scaffold and its derivatives are known for a broad spectrum of biological activities, including antibacterial, antifungal, antiviral, and anticancer properties **[1–4]**. Modulation of the anionic state can have profound implications for drug design by affecting solubility, membrane permeability, protein binding, and overall molecular recognition **[11–13,20]**. In organic synthesis, the anionic forms of isatin derivatives are valuable intermediates for constructing complex architectures via nucleophilic additions, condensations, and cyclization reactions **[8,11–14,16]**. Controlling the deprotonation and reactivity parameters of isatin anions is crucial for chemo- and regioselective functionalizations, thereby enabling the development of new synthetic methodologies **[12–14,18,29]**. Furthermore, in materials science, the electrical and optical properties of isatin-based molecules can be fine-tuned by varying substituents and charge states, making them promising candidates for applications in optoelectronic devices and advanced functional materials **[7,14–15,22,30]**.

This study focuses on a comprehensive investigation of the anionic forms of isatin and its halogenated derivatives **[11–13,16–19]**. By employing a combination of computational techniques, we elucidate the relative energy profiles, thermochemistry, and key reactivity parameters of these anions **[9–10,16–18,28–29]**. By theoretical approaches, we aim to deepen the understanding of how halogen substitution and anionic states modulate molecular properties and reactivity **[8–10,16–20]**. Such insights will pave the way for developing isatin-based frameworks with enhanced therapeutic potential, improved synthetic utility, and novel functionalities in advanced materials **[3–4,14–15,22,30]**.

II.COMPUTATIONAL DETAILS

Anionic forms of the enol conformer of isatin and its halogen derivatives are explored for relative energy calculations in gas phase. The numbering scheme of the anions of isatin and its halogen derivatives is shown in Figure 1. The geometry optimized anions of isatin and its halogenated derivatives using density functional B3LYP/6-311++G** calculations are shown in Figure 2 [**27-31**]. Thermodynamic properties such as enthalpies, and Gibbs energies were calculated at 298.15 K and 1 atm pressure. All computations were performed using the Gaussian 09 packages [**32**].

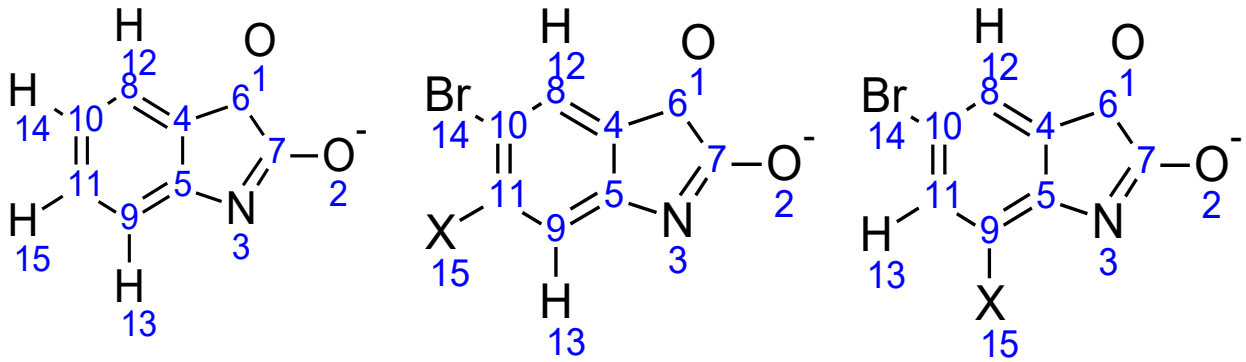

Figure 1 Numbering scheme of enol form of anions of Isatin (1a), 10-Bromo-11-haloisatin (1b), 10-Bromo-9-haloisatin (1c)

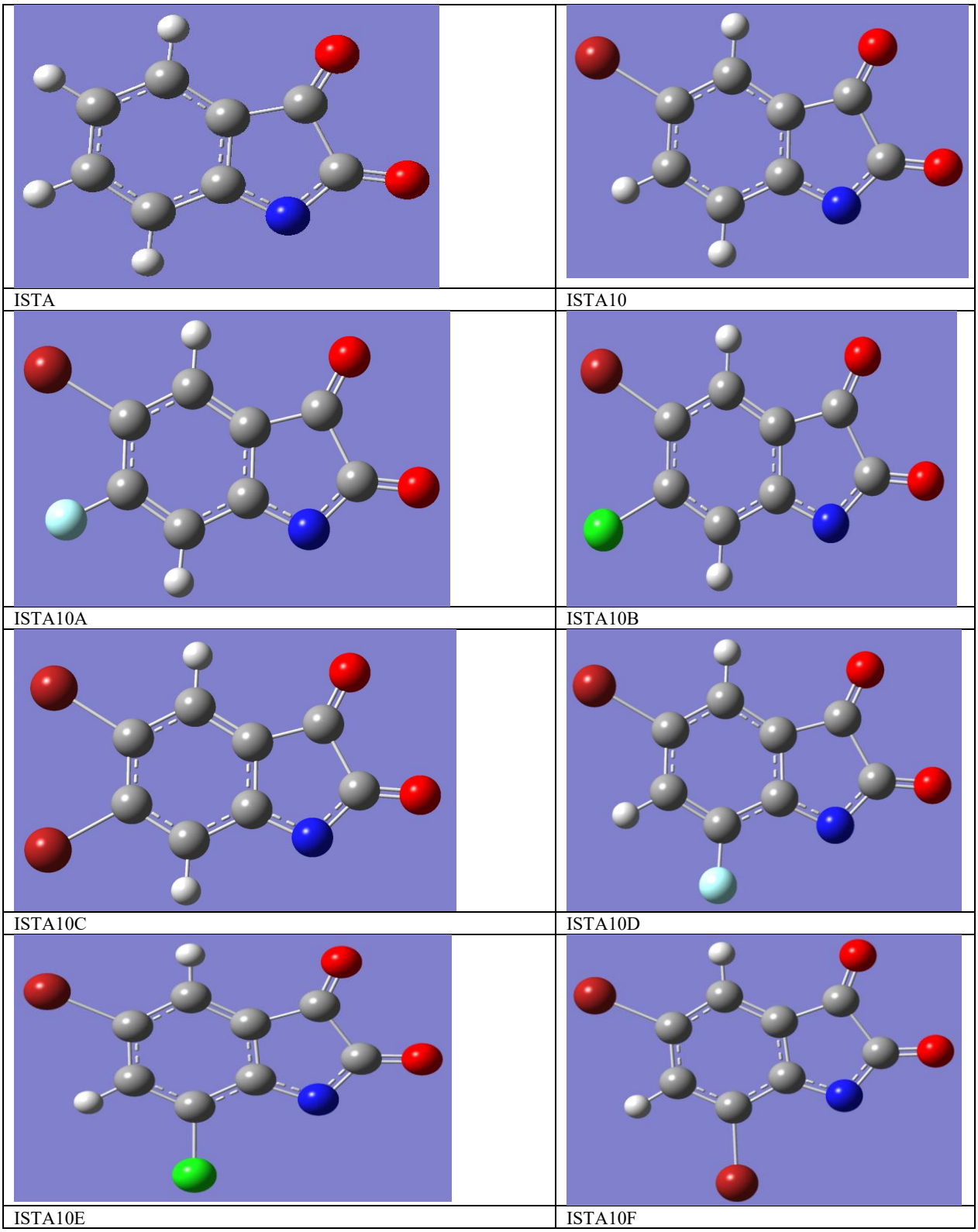

Figure 2 B3LYP/6-311G**++ geometry optimized tautomers and conformers of anions of enol form of isatin and its halogen derivatives [Color Code: Carbon (Grey), Hydrogen (White), Oxygen (Red), Nitrogen (Blue), Fluorine (Light Blue), Chlorine (Green), Bromine (Dark Red)]

III.RESULTS AND DISCUSSION

3.1 Relative Energies in Gas Phase

The relative energies of the low-energy conformers of the anionic forms of isatin and its halogenated derivatives are summarized in Table 1 [19]. Analysis of the computed total energies reveals that the parent isatin anion (ISTA) exhibits a very high relative energy (3229860.869 kcal mol^{-1}), indicating significantly lower stability compared to its halogen-substituted analogs. This clearly suggests that halogen substitution enhances the stability of the isatin anion. The ISTA10 series (ISTA10 through ISTA10F) displays progressively lower total energies, with ISTA10F showing the minimum energy value (−3551497.145 kcal mol^{-1}); therefore, ISTA10F was selected as the reference conformer (ΔE = 0 kcal mol^{-1}). Among these species, ISTA10C and ISTA10F exhibit extremely low relative energies (2.1908 and 0 kcal mol^{-1}, respectively), demonstrating that these brominated analogs are the most stable within the series. The enhanced stability associated with bromine substitution, particularly at the C-9 position, indicates that heavier halogens impart greater stabilization than lighter ones.

Zero-point vibrational energy (ZPVE) analysis further supports these observations. ISTA exhibits the highest ZPVE (62.471 kcal mol^{-1}), whereas the halogen-substituted derivatives show lower ZPVE values, consistent with increased molecular flexibility. Substitution at the C-9 and C-11 positions results in decreased ZPVE, implying greater vibrational freedom and reduced molecular rigidity. This trend correlates with the decreasing electronegativity of the halogen substituents; heavier halogens with larger, more diffuse p-orbitals participate less effectively in +R resonance interactions with the isatin ring, promoting non-planarity and conformational flexibility. Consequently, the dibromo derivative at the C-11 position exhibits the highest flexibility due to reduced resonance stabilization and steric repulsion between adjacent bromine atoms. Such flexibility is highly relevant in medicinal chemistry, as molecular rigidity versus flexibility can significantly influence biological recognition, binding efficiency, and pharmacokinetic behavior.

Table 1 Relative energy of anions of enolic conformer of isatin and its halogen derivatives

SPECIES	E (Kcal/mol)	ZPVE (Kcal/mol)	E_{tot} (Kcal/mol)	Relative Energy (Kcal/mol)
ISTA	-321699	62.47115582	-321636.2758	3229860.869
ISTA10	-1936624.011	56.19470753	-1936567.816	1614929.329
ISTA10A	-1998916.913	51.17122582	-1998865.742	1552631.403
ISTA10B	-2225041.393	50.22464377	-2224991.169	1326505.977
ISTA10C	-3551544.753	49.79898458	-3551494.954	2.19083508
ISTA10D	-1998914.974	51.14967421	-1998863.825	1552633.32
ISTA10E	-2225042.764	50.33590818	-2224992.428	1326504.717
ISTA10F	-3551547.04	49.89474209	-3551497.145	0

3.2 Thermochemistry

Analysis of the thermochemical data presented in Table 2 [**19**] reveals that the formation of anionic species is thermodynamically more favorable for halogen-substituted isatins compared to unsubstituted isatin. Among the halogenated derivatives, deprotonation leading to anions derived from the *enol-1* and *enol-2* conformers [**19**] becomes increasingly favorable as the electronegativity of the halogen decreases, as evidenced by progressively lower ΔH_1 and ΔH_2 values. For most halogenated systems, ΔH_1 and ΔH_2 values are less positive when substitution occurs at the C-11 position relative to the C-9 position, with the exception of the brominated derivatives. In the case of dibromo-substituted analogues, ΔH_1 and ΔH_2 values are instead lower for substitution at the C-

9 position, suggesting enhanced stabilization by bromine at this site.

Trends in the Gibbs free energy changes (ΔG_1 and ΔG_2) further support these observations. ΔG values decrease with decreasing halogen electronegativity, and deprotonation at the C-9 position is generally more favorable than at C-11. Overall, dibromo derivatives substituted at the C-9 and C-11 positions exhibit the most favorable ΔH and ΔG values, indicating enhanced thermodynamic preference for anion formation. Additionally, for most halogenated isatin derivatives, deprotonation from the *enol-2* conformer [**19**] is more favorable, as reflected by consistently lower ΔG_2 values, with the sole exception being the 9-fluoro derivative (ISTA10D).

Table 2 ΔH˚ and ΔG˚ values in Kcal/mol for formation of anion from enol1 and enol2 conformers

SPECIES	ΔH1 (Kcal/mol)	ΔG1 (Kcal/mol)	ΔH2 (Kcal/mol)	ΔG2 (Kcal/mol)
ISTA	320.5391273	320.6621191	320.6614916	320.7499703
ISTA10	315.0791715	315.0521886	315.1086644	315.0603462
ISTA10A	311.7150958	311.7922794	311.7201158	311.7709441
ISTA10B	311.6109293	311.6197144	311.5864564	311.5682586
ISTA10C	311.4741323	311.4998602	311.4145189	311.4245591
ISTA10D	311.9679819	311.5632386	311.9849246	311.5644936
ISTA10E	310.8541534	310.440625	310.8579185	310.4268198
ISTA10F	310.4268198	310.0578445	310.4067395	310.0390192

3.3 Global Reactivity Parameters

Understanding the intrinsic electronic properties of molecular systems is essential for predicting their chemical behavior, reactivity, and stability. Global reactivity parameters (GRPs) derived from frontier molecular orbital theory and density functional theory (DFT) as given in Table 3 provide valuable insights into the electronic structure and potential reactivity pathways of organic molecules [**37-39**]. Key descriptors such as the highest occupied molecular orbital (HOMO) and lowest unoccupied molecular orbital (LUMO) energies, HOMO–LUMO energy gap (ΔE), dipole moment, electronegativity (χ), chemical potential (μ), chemical hardness (η), global softness (S), electrophilicity index (ω), and nucleophilicity index (N) serve as quantitative tools for evaluating nucleophilic and electrophilic tendencies, charge-transfer susceptibility, and kinetic stability of molecular species **[35-38]**.

According to Koopmans' theorem and conceptual DFT, HOMO and LUMO energies are fundamentally related to ionization potential and electron affinity [**33,35-36**], enabling estimation of electronegativity, hardness, and electrophilicity **[37–40]**. A lower HOMO–LUMO energy gap generally corresponds to higher chemical reactivity and lower kinetic stability, whereas a larger gap indicates enhanced stability and lower reactivity **[38,42]**. Chemical hardness and softness, as introduced by Pearson within the hard-soft acid–base (HSAB) principle, describe the resistance of a system to charge transfer and polarization **[35,38]**. The global electrophilicity index proposed by Parr is an effective descriptor for identifying electrophilic character [**36**], while recent developments in conceptual DFT have introduced global nucleophilicity scales to complement electrophilicity and assess nucleophile strength **[39]**.

Thus, GRPs offer a comprehensive theoretical framework to rationalize and compare the reactivity of neutral and anionic species of isatin and its derivatives, contributing to a deeper understanding of their chemical behavior and potential applications in pharmaceutical and material-based systems.

Table 3 Global Reactivity Parameters of anions of enolic conformer of isatin and its halogen derivatives

SPECIES	D.M (Debye)	HOMO (ha)	LUMO (ha)	HLG (ha)	X (ha)	μ (ha)	η (ha)	S (ha^{-1})	N (ha)	ω (ha)
ISTA	7.5928	-0.05729 (38)	0.0515	0.10879	0.002895	-0.002895	0.054395	18.3839	0.29138	7.70386E-05
ISTA10	11.3437	-0.06895 (55)	0.03748	0.10643	0.015735	-0.015735	0.053215	18.7908	0.27972	0.00232632
ISTA10A	10.9136	-0.07637 (59)	0.03543	0.1118	0.02047	-0.02047	0.0559	17.8910	0.2723	0.003747951
ISTA10B	11.4279	-0.07822 (63)	0.02995	0.10817	0.024135	-0.024135	0.054085	18.4862	0.27045	0.005385026
ISTA10C	12.8021	-0.07903 (72)	0.02848	0.10751	0.025275	-0.025275	0.053755	18.6060	0.26964	0.005942011
ISTA10D	11.3275	-0.07495 (59)	0.03059	0.10554	0.02218	-0.02218	0.05277	18.9532	0.27372	0.004661289
ISTA10E	10.8725	-0.07481 (63)	0.02719	0.102	0.02381	-0.02381	0.051	19.6078	0.27386	0.005558001
ISTA10F	10.6681	-0.07997 (72)	0.0258	0.10577	0.027085	-0.027085	0.052885	18.9121	0.2687	0.006935778

3.3.1 Dipole Moment (DM)

The dipole moments as reported in Table 3 of the studied species range from 7.5928 Debye for ISTA to 12.8021 Debye for ISTA10C, indicating that ISTA10C is the most polar molecule, whereas ISTA exhibits the lowest polarity [9,10,16-18]. Comparison of dipole moments across the series reveals that bromine substitution at the C-10 position of the isatin anion results in a substantial increase in molecular polarity [8-10,15,20]. Substitution at the C-11 position of ISTA10 also enhances polarity, which can be attributed primarily to the inductive (−I) effect outweighing the resonance (+R) effect for most halogens [8,15,20]. An exception is observed for fluorine, where the +R effect becomes dominant due to effective 2p–2p orbital overlap between carbon and fluorine [20,35].

Conversely, halogen substitution at the C-9 position leads to a decrease in polarity, likely due to reduced steric hindrance and improved planarity, which facilitates efficient conjugative (+R) interaction between the halogen and the carbonyl system [9-10,16-17]. Fluorine again deviates from this trend; at the C-9 position, its strong −I effect surpasses the +R effect, resulting in enhanced polarity relative to other halogens at the same position [15,20,35].

3.3.2 HLG (HOMO LUMO Gap)

The HOMO–LUMO energy gap in Table 3 represents a key quantum chemical descriptor, reflecting the energy difference between the Highest Occupied Molecular Orbital (HOMO) and the Lowest Unoccupied Molecular Orbital (LUMO) [9-10,16,20]. A larger HOMO–LUMO gap is typically associated with greater molecular stability and reduced chemical reactivity, whereas a smaller gap signifies enhanced reactivity and lower kinetic stability [33,35,38]. The parent ISTA anion exhibits a HOMO–LUMO gap of 0.10879 ha, suggesting comparatively higher stability. Among its halogenated derivatives (ISTA10, ISTA10A, ISTA10B, ISTA10C, ISTA10D, ISTA10E, and ISTA10F), the energy gaps range from 0.1020 ha (ISTA10E) to 0.1118 ha (ISTA10A). The largest gap observed for ISTA10A (0.1118 ha) indicates that it is the most electronically stable derivative in the series, whereas the smallest gap observed for ISTA10E (0.102 ha) suggests a higher potential for chemical reactivity and lower stability [9,10,20].

Further analysis reveals that bromination at the C-10 position of the isatin anion leads to a reduction in the HOMO–LUMO gap, indicating an increase in reactivity [8-10,15]. In contrast, fluorination at the C-11 position of ISTA10 results in a wider gap, implying reduced reactivity and enhanced molecular stability [20,35]. Additionally, for dihalo-substituted derivatives, the reactivity is comparatively lower when the halogen is positioned at C-11 rather than C-9, reflecting the positional influence of halogen substitution on the electronic properties of the isatin scaffold [9,16-17].

3.3.3 Electronegativity (χ)

A clear increasing trend in electronegativity in Table 3 is observed from ISTA to ISTA10F, indicating a

progressive enhancement in electron-attracting ability across the series [33,35,38]. This suggests that the halogen-substituted anions exhibit a stronger tendency to withdraw electron density compared to the unsubstituted ISTA anion [8-10,15]. Among the derivatives, ISTA10C and ISTA10F display the highest electronegativity values, reflecting the strong electron-withdrawing influence of bromine substituents [15,20]. The exceptionally high electronegativity of ISTA10F implies that it is likely to be highly reactive as electrophilic species.

Anions possessing higher electronegativity (such as the ISTA10 series) are expected to engage more strongly in interactions with electron-rich or less electronegative systems [33,35-37]. This enhanced electron-accepting behavior can significantly influence their physicochemical characteristics, including the formation of stronger hydrogen-bond interactions and increased affinity toward coordination with metal ions. Such properties may have important implications for their reactivity, stability, and potential applications in supramolecular, catalytic, and biological environments [14,15,37].

3.3.4 Chemical Potential (μ)

The chemical potential values reported in Table 3 are negative for all species, indicating that the anionic forms of isatin and its halogenated derivatives possess an inherent thermodynamic tendency to accept additional electron density rather than donate it [33,35-38]. Within the framework of conceptual density functional theory, this behavior reflects the stability of these anions toward electron loss and their potential participation in electron-accepting (reduction-type) processes [33,36-37]. A systematic increase in the magnitude of chemical potential is observed from ISTA to ISTA10F, closely paralleling the trend in electronegativity, consistent with the fundamental relation $\mu = -\chi$ [33,35].

Halogen substitution leads to progressively more negative chemical potential values, signifying enhanced electron-accepting ability of the anionic species [9-10,15,20]. In particular, bromination at the C-10 position results in a noticeable increase in the magnitude of μ, indicating that ISTA10 exhibits a stronger tendency to accommodate excess electron density compared to the unsubstituted ISTA anion [8-10,15]. Furthermore, an increase in chemical potential magnitude is observed with increasing electronegativity of the halogen substituent at the C-9 and C-11 positions. For the ISTA10 series, chemical potential values are generally more negative for substitution at the C-9 position than at the C-11 position, suggesting a stronger electronic influence of the halogen when positioned closer to the anionic center, leading to more efficient charge stabilization [16-17].

Chemical potential also serves as an important descriptor of molecular reactivity. Species with larger magnitudes of chemical potential are generally more reactive in electron-accepting pathways and are more susceptible to charge-transfer interactions. In this context, ISTA, which exhibits the least negative chemical potential, may be considered relatively less reactive and electronically more rigid compared to its halogen-substituted counterparts. The more negative chemical potential values of halogenated isatin anions therefore indicate enhanced reactivity and greater propensity for participation in redox processes, catalytic environments, and polar reaction mechanisms. Overall, these trends demonstrate that halogen identity and substitution position provide an effective means of tuning the electron-accepting character and reactivity of isatin-based anions.

3.3.5 Chemical Hardness (η)

Chemical hardness (η) presented in Table 3 describes the resistance of a molecule to deformation or polarization of its electron density and is therefore closely associated with molecular stability and reactivity [35,38]. Higher chemical hardness corresponds to greater stability and lower chemical reactivity, whereas lower hardness reflects enhanced reactivity and reduced stability [33,35]. The parent isatin anion (ISTA) exhibits a chemical hardness of 0.054395 ha. Among the halogen-substituted derivatives, ISTA10A shows the highest chemical hardness (0.0559 ha), indicating that it is the most stable and least reactive member of the series [9,10,20].

Introduction of bromine at the C-10 position decreases the hardness of ISTA, suggesting that bromination enhances the ease of electronic polarization and therefore increases the reactivity of ISTA10. In contrast, substitution with fluorine at the C-11 position increases chemical hardness, primarily due to fluorine's strong electronegativity and the associated steric and electronic effects, which limit distortion of the electron cloud. As the electronegativity of the halogens decreases from F to Br, chemical hardness likewise decreases, as seen across the ISTA10A → ISTA10C trend [15,35].

Furthermore, halogen substitution at the C-9 position results in lower hardness than substitution at C-11, due to reduced steric hindrance at C-9, which allows for easier electron-density redistribution. ISTA10E displays the lowest chemical hardness value (0.051 ha), indicating that it is the most reactive and least stable derivative. This can be attributed to an optimal balance between electronegativity and steric effects, which facilitates electron cloud distortion and enhances chemical reactivity [16,17].

3.3.6 Global Softness (S)

Global softness (S) presented in Table 3 quantifies the ease with which the electron density of a molecule can be polarized. It is the reciprocal of chemical hardness, and therefore reflects molecular reactivity [33,35,38]. Higher global softness values correspond to greater chemical reactivity and lower thermodynamic stability, whereas lower softness values indicate enhanced stability and reduced reactivity. Among the derivatives studied, ISTA10E exhibits the highest global softness value (19.6078 ha^{-1}), signifying that it is the most reactive and least stable species in the series. Conversely, ISTA10A shows the lowest global softness value (17.8910 ha^{-1}), indicating the highest stability and lowest reactivity among the derivatives. These observations are fully consistent with the chemical hardness trends, further validating the inverse relationship between softness and hardness [9-10,20].

3.3.7 Global Electrophilicity Index (ꝯ)

Global electrophilicity index reported in Table 3, is a quantitative measure of molecule's electrophilicity or probability to accept electrons [36]. From Table 9, it is clear that ISTA10 has the lowest electrophilicity among all eight species. The introduction of halogen in ISTA10 increases its electrophilicity due to their -I effect leading to more rise in LUMO energy than HOMO [15,20,36]. Halogen substitution of ISTA10 show more increase in electrophilicity if it is placed at 9th position rather than 11th except for fluorine derivative and also it has highest value for dibromo derivatives despite the fact that -Br is least electronegative. The trend in electrophilicity values indicate that lesser the electron withdrawing effect of halogen, more is the electrophilicity indicating that energy of HOMO rises more than LUMO [15,35-36].

3.3.8 Global Nucleophilicity Index (N)

The global nucleophilicity index (N), calculated relative to tetracyanoethylene, provides a quantitative measure of electron-donating ability [39].

The global nucleophilicity index (N) was calculated using the empirical relation:

$$N = HOMO_{compound} - HOMO_{TCN}$$

HOMO of TCN = -0.34867 ha

where tetracyanoethylene (TCN) is used as the reference electrophile and its HOMO value is

Halogen substitution significantly influences the electron density distribution and, consequently, the nucleophilicity index (N) given in Table 3. The unsubstituted isatin anion exhibits the highest nucleophilicity, whereas halogenation progressively decreases nucleophilicity due to the electron-withdrawing nature of halogens [15,39]. As the halogen substituent changes from fluorine to bromine at the C-11 position in ISTA10, a gradual decrease in nucleophilicity is observed. This trend can be attributed to increased steric bulk and reduced resonance (+R) participation of heavier halogens, which diminishes electron donation toward the anionic center.

However, when substitution occurs at the C-9 position, the proximity of the halogen to the anionic center allows greater resonance donation (+R effect), particularly for bromine, which faces lower steric repulsion at this position. As a result, derivatives such

as ISTA10D and ISTA10E exhibit higher nucleophilicity compared to their C-11 substituted counterparts, ISTA10A and ISTA10B. In contrast, for the dibrominated species, ISTA10F shows lower nucleophilicity than ISTA10C. This reduction can be attributed to strong interelectronic repulsion between the bromine atom at C-9 and the anionic center, which destabilizes electron density donation, thereby lowering nucleophilicity relative to ISTA10C [16-17,39].

IV.CONCLUSIONS

A comprehensive density functional theory investigation has been carried out on the enol-derived anionic forms of isatin and its halogen-substituted derivatives to elucidate the influence of halogen identity and substitution position on stability, thermodynamics, and electronic reactivity. Relative energy and ZPVE analyses demonstrate that halogen substitution markedly stabilizes the isatin anion, with brominated derivatives—particularly those substituted at the C-9 and C-11 positions—exhibiting the lowest energies and enhanced conformational flexibility. The reduced ZPVE values for halogenated systems indicate increased vibrational freedom, highlighting the role of heavier halogens in modulating molecular rigidity through steric and resonance effects.

Thermochemical analysis further reveals that anion formation becomes progressively more favorable upon halogen substitution, as reflected by decreasing $\Delta H°$ and $\Delta G°$ values. Dibromo-substituted derivatives show the highest thermodynamic preference for deprotonation, underscoring the combined inductive and polarizability effects of bromine in stabilizing the anionic state. Position-dependent trends indicate that substitution at the C-9 position generally provides greater stabilization than substitution at C-11, particularly for brominated systems, emphasizing the importance of proximity to the anionic center in charge delocalization.

Global reactivity parameters derived from conceptual DFT provide deeper insight into the electronic modulation induced by halogen substitution. Systematic variations in HOMO–LUMO gaps, electronegativity, chemical potential, hardness, softness, electrophilicity, and nucleophilicity reveal that halogenation enhances the electron-accepting character and reactivity of isatin anions. The increasingly negative chemical potential values from ISTA to ISTA10F confirm a growing tendency toward electron acceptance, while hardness–softness trends identify ISTA10E as the most chemically soft and reactive species. Electrophilicity increases and nucleophilicity decreases upon halogen substitution, reflecting the dominant electron-withdrawing influence of halogens, with clear positional effects distinguishing C-9 and C-11 substitution patterns.

While previous studies have largely focused on neutral isatin derivatives or isolated anionic species, the present work constitutes the *first systematic and position-resolved DFT investigation of enol-derived anionic forms of mono- and dihalogenated isatins*. By integrating relative stability, thermochemical feasibility of anion formation, and a complete global reactivity descriptor analysis across an entire family of halogenated isatin anions, this study fills a critical gap in the theoretical understanding of isatin chemistry. The clear correlations established between halogen identity, substitution position, and electronic reactivity provide a rational framework for tuning the stability and reactivity of isatin-based anions.

Overall, the findings not only advance fundamental insight into the electronic structure and reactivity of halogenated isatin anions but also offer valuable guidance for the rational design of isatin-based frameworks with tailored properties for applications in organic synthesis, medicinal chemistry, and functional material development.

ACKNOWLEDGEMENT

Authors are thankful to Shyama Prasad Vidyalaya Lodi Estate and Amit Kumar, Department of Chemistry, University of Delhi for supporting this work

REFERENCES

[1] Medvedeva, N. I.; *et al.* Isatin and its derivatives: A review on their chemistry and biological activity. Eur. J. Med. Chem. *2021*, 223, 113632.

[2] Vine, K. L.; Locke, J. M.; *et al.* The medicinal chemistry and biological activity of isatin and its derivatives. Bioorg. Med. Chem. *2009*, 17, 3295–3315.

[3] Bansal, Y.; Silakari, O. Isatin: A versatile scaffold for drug discovery. Chem. Biol. Drug Des. *2017*, 89, 243–256.

[4] Pandeya, S. N.; *et al.* Synthesis and antimicrobial activity of isatin derivatives. Acta Pharm. *2005*, 55, 27–46.
[5] Popp, F. D. The chemistry of isatin. Chem. Rev. *1973*, 73, 129–145.
[6] Kołaczek, A.; *et al.* Isatin derivatives in modern organic synthesis. Adv. Synth. Catal. *2020*, 362, 2444–2467.
[7] Patel, H.; *et al.* Isatin-based heterocycles for materials and sensor applications. ACS Omega *2024*, 9, 1024–1035.
[8] Samadhiya, P.; Srivastava, D. Halogenated isatin derivatives: synthesis, chemistry, and biological significance. J. Heterocycl. Chem. *2018*, 55, 1823–1835.
[9] Xu, J.; *et al.* Electronic structure and substituent effects in isatin derivatives: A computational study. J. Mol. Struct. (THEOCHEM) *2012*, 913, 241–247.
[10] Zhang, T.; *et al.* Substituent effects on the reactivity of isatin derivatives via DFT calculations. Comput. Theor. Chem. *2019*, 1167, 112631.
[11] Ishida, T.; *et al.* Anionic intermediates in isatin-based reactions: Mechanistic insights. J. Org. Chem. *2016*, 81, 8955–8964.
[12] Yu, L.; *et al.* Deprotonation behavior and resonance stabilization of isatin derivatives: Spectroscopic and computational investigation. J. Phys. Chem. A *2018*, 122, 5105–5114.
[13] Liu, Y.; *et al.* Reactivity of isatin anions in nucleophilic addition reactions. Org. Biomol. Chem. *2022*, 20, 417–425.
[14] Liang, C.; *et al.* Halogen-substituted isatin derivatives as multifunctional pharmacophores. Eur. J. Med. Chem. *2023*, 257, 115444.
[15] Ali, A.; *et al.* Halogenated indoles and isatins in medicinal chemistry. RSC Adv. *2020*, 10, 35705–35730.
[16] Singh, S.; *et al.* Theoretical investigation of isatin derivatives: DFT and NBO analysis. J. Mol. Struct. *2016*, 1120, 32–41.
[17] Gupta, A.; *et al.* Electronic structure and charge distribution analysis in indole-based systems. Comput. Theor. Chem. *2020*, 1187, 112953.
[18] Tesfaye, F.; *et al.* Molecular structure, NBO charge distribution, and reactivity descriptors of heterocycles. J. Mol. Graphics Modell. *2022*, 115, 108219.
[19] Arora, E. Theoretical study of isatin and its halogenated derivatives. J. Emerg. Technol. Innov. Res. *2024*, 11, h113–h136.
[20] Zhang, J.; *et al.* Halogen substitution effects on HOMO–LUMO gaps and bioactivity of indole frameworks. RSC Adv. *2021*, 11, 31490–31502.
[21] Jatav, V.; *et al.* Synthesis and spectral characterization of isatin-based Schiff bases. Indian J. Chem., Sect. B *2007*, 46, 1973–1978.
[22] Silverstein, R. M.; Webster, F. X.; Kiemle, D. J. *Spectrometric Identification of Organic Compounds*, 8th ed.; Wiley: New York, 2014.
[23] Perrin, D. D.; Dempsey, B. *Buffers for pH and Metal Ion Control*; Springer: Dordrecht, 1974.
[24] Kolmacková, J.; *et al.* Acid–base behavior of indole derivatives: Experimental and computational pKa study. J. Phys. Chem. B *2021*, 125, 7539–7550.
[25] Gao, J.; *et al.* Substituent effects on acidity of heterocycles via computational pKa prediction. J. Chem. Theory Comput. *2019*, 15, 2629–2640.
[26] Ghosh, R.; *et al.* Isatin-based organic semiconductors for optoelectronic applications. Dyes Pigments *2022*, 204, 110477.
[27] Becke, A. D. Density-functional thermochemistry. III. The role of exact exchange. J. Chem. Phys. *1993*, 98, 5648–5652.
[28] Lee, C.; Yang, W.; Parr, R. G. Development of the Colle–Salvetti correlation-energy formula into a functional of the electron density. Phys. Rev. B *1988*, 37, 785–789.
[29] Hariharan, P. C.; Pople, J. A. The influence of polarization functions on molecular orbital hydrogenation energies. Theor. Chim. Acta *1973*, 28, 213–222.
[30] McLean, A. D.; Chandler, G. S. Contracted Gaussian basis sets for molecular calculations. I. Second-row atoms, Z = 11–18. J. Chem. Phys. *1980*, 72, 5639–5648.
[31] Clark, T.; Chandrasekhar, J.; Spitznagel, G. W.; Schleyer, P. v. R. Efficient diffuse function-augmented basis sets for anion calculations. J. Comput. Chem. *1983*, 4, 294–301.
[32] Frisch, M. J.; *et al. Gaussian 09*, Revision D.01; Gaussian, Inc.: Wallingford, CT, 2009.
[33] Parr, R. G.; Yang, W. *Density-Functional Theory of Atoms and Molecules*; Oxford University Press: Oxford, 1989.

[34] Fukui, K. *Theory of Orientation and Stereoselection*; Springer-Verlag: Berlin, 1975.
[35] Pearson, R. G. Absolute electronegativity and hardness: Application to organic chemistry. J. Org. Chem. *1989*, 54, 1423–1430.
[36] Parr, R. G.; Szentpály, L. V.; Liu, S. Electrophilicity index. J. Am. Chem. Soc. *1999*, 121, 1922–1924.
[37] Ghiringhelli, L. M.; *et al.* Chemical reactivity indexes in conceptual DFT. Chem. Rev. *2022*, 122, 356–427.
[38] Chattaraj, P. K.; Maiti, B.; Sarkar, U. Conceptual DFT based electronic structure principles. J. Chem. Educ. *2009*, 86, 1395–1403.
[39] Domingo, L. R.; Aurell, M. J.; Pérez, P.; Contreras, R. Understanding the nucleophilicity index. Org. Biomol. Chem. *2016*, 14, 7160–7172.